Numerical investigation of the effect of Froude number on flow pattern around a submerged T-shaped spur dike in a 90° bend

Mohammad VAGHEFI[1,*], Mohammad SHAKERDARGAH[2], Maryam AKBARI[1]
[1]Department of Civil Engineering, Persian Gulf University, Bushehr, Iran
[2]Department of Civil Engineering, Islamic Azad University, Bushehr, Iran

Abstract: A spur dike is a structure that projects from a stream bank into the river channel and causes a redirection of flow away from the bank toward the tip of the spur dike. Construction of a spur dike against the flow causes significant changes in flow pattern in the channel. In this study, the flow pattern around a 25% submerged T-shaped spur dike in a 90° bend with rigid bed and various Froude numbers 0.2, 0.34, 0.45, and 0.6 was examined using FLOW-3D software. Numerical results were compared with experimental results and analyzed. The results indicated that in cross section around the spur dike, when Froude number increases, the formed vortexes decreased by 35%. Longitudinal velocity and lateral velocity increased twice as much as their former values. The highest amount of vertical velocity was observed between the wing of the spur dike and the external bend, and closer to the external bend, with an increase in Froude number, vertical velocity components variations decreased by 33%. Moreover, the results indicated that when the Froude number increases, the width of the separation zone increases, but the change in the length of the separation zone in different levels is negligible.

Key words: Submerged T-shaped spur dike, Froude number, flow pattern, 90° bend, FLOW-3D

1. Introduction

Rivers have several bends as they run through nature. Generally, it is assumed that the force affecting the flow in river bends is centrifugal force. Because of centrifugal force and its interaction with lateral gradients of the pressure from the lateral slope of the water's surface, a secondary current is formed. In addition, because of the interaction among secondary currents and because the velocity profile is not constant in depth, helical flow appears.

A spur dike may be defined as a structure extending outward from the bank of a river for the purpose of deflecting the current away from the bank to protect it from erosion. In many instances, impaired streams and rivers often erode the banks and move laterally, resulting in land loss, channel change, excessive sediment yield, and degradation of the water quality. For economic reasons, spur dikes are often constructed of riprap and are commonly designed to be submerged during high flows [1]. Too much scour in the outer banks of rivers, because of secondary currents and helical flows, is an important matter in river engineering.

Using spur dikes has been an indirect way to protect the banks of rivers. Because spur dikes are simple structures, are easy to implement, and are economical, they have attracted much attention. Many studies concerning flow pattern and scour in rivers have been carried out to date. Some of them are mentioned as follows.

*Correspondence: vaghefi52@gmail.com

Ahmad, in 1951–1953, studied flow patterns around impermeable groins. He located spur dikes in different angles ranging from $30°$ to $150°$ in proportion to the upstream bed in a straight flume and observed that at an angle wider than $90°$ relative velocity of the flow decreases [2,3]. Gill, in 1972, in an experiment proved that the distance between spur dikes depends much on the radius of curvature. In nearly straight routes, the distance between spur dikes is about 5 times the length of the spur dike, whereas in bends it is equal to or twice the length of the spur dike [4]. Rajaratnam and Nwachukwu, in 1983, studied the structure of turbulent flow near a groin. Based on experimental observations, the deflected flow was analyzed using the model of the three-dimensional turbulent boundary layer [5,6]. Soliman et al., in 1997, introduced a two-dimensional mathematical model for studying the effects of spur dikes on the Nile River's bend's morphology. They used different lengths and distances of spur dikes for this study in order to assess their effect on the level of water surface and velocity components [7]. Blanckaert and Graf, in 2001, conducted an experimental study on a $120°$ bend channel and measured secondary flow and maximum velocity at the $60°$ cross section [8]. Booij, in 2003, using large eddy simulation (LES), simulated flow field in a $180°$ bend and measured Reynolds shear stress [9]. Giri et al., in 2004, carried out experimental and numerical simulations of flow and turbulence in a bend channel with unsubmerged spur dikes. They measured flow velocity by changing the position of spur dikes, and measured vortex field and turbulence intensity two-dimensionally [10]. Nagata et al., in 2005, carried out a numerical simulation of the three-dimensional flow pattern around a single spur dike with a live bed. They analyzed average flow and studied its relation with the way a scour hole is created and expands [11]. Fazli et al., in 2008, performed an experimental study on a $90°$ bend channel to study the parameters affecting scour around short and straight spur dikes. The results of the study on a bend channel with a single spur dike indicated that in developed bends, as the spur dike is moved away from the beginning of the bend, maximum depth of scour rises, whereas this parameter in a steep bend first decreases and then increases [12]. Ghodsian and Vaghefi, in 2009, carried out an experimental study on how changes in Froude number, and the length of the wing and web of T-shaped spur dike located in a $75°$ position affect flow pattern in a $90°$ bend. They proved that as the length of the spur dike increases, the length of separation zone and the formed vortex in the zone increases [13]. Duan, in 2009, investigated average and turbulent flow around a straight spur dike located in an experimental channel with a rigid bed. She observed that average flow in both lateral and vertical directions separated, and in the circulation zone behind the spur dike there is a combination of horizontal and vertical vortexes [14]. Yazdi et al., in 2010, simulated the flow pattern around a single spur dike in a straight route using the k-ε model in Fluent software. They studied the effect of discharge, and length and angle of the spur dike on shear stress distribution [15]. Since 2008, Vaghefi et al. have experimentally investigated the flow pattern and scour around an unsubmerged T-shaped spur dike in a $90°$ bend in different parameters including Froude number, curvature radius, spur dike position, spur dike geometry, the effect of time, flow conditions etc. [16–18]. Acharya et al., in 2013, carried out a three-dimensional numerical investigation of the turbulent flow pattern around a series of straight spur dikes located in a straight route with a live and fixed bed, using FLOW-3D software. They used the k-ε turbulence model for modelling and compared the results with experimental results [19].

Because few studies have been carried out on flow patterns around submerged spur dikes located in bends, the effect of Froude number on the flow pattern around a submerged T-shaped spur dike located in a $90°$ bend was studied numerically and was compared with the results of experimental modelling.

2. Experimental model introduction

The intended experiments were carried out by Vaghefi [16] in the Hydraulics Laboratory of Tarbiat Modares University in Iran, on a laboratory flume 60 cm wide and 70 cm high in a compound of direct and bend routes. The straight upstream route is 710 cm long and is connected to a straight downstream route 520 cm long via a 90° bend with an external radius of 270 cm and an internal radius of 210 cm. The ratio of bend radius to width of channel is 4. Uniform sediments have an average diameter of 1.28 mm. The flow discharge throughout the experiment is held constant and equals 25 L/s. The spur dike used in this experiment is a T-shaped Plexiglas spur dike. The length of the wing (L) and that of the web (l) are the same and equal to 9 cm, and the height is 25 cm. This spur dike is vertical and unsubmerged in a 45° position, and is located in the external bend. The features of the laboratory flume and the schematic view of the T-shaped spur dike are presented in Figure 1.
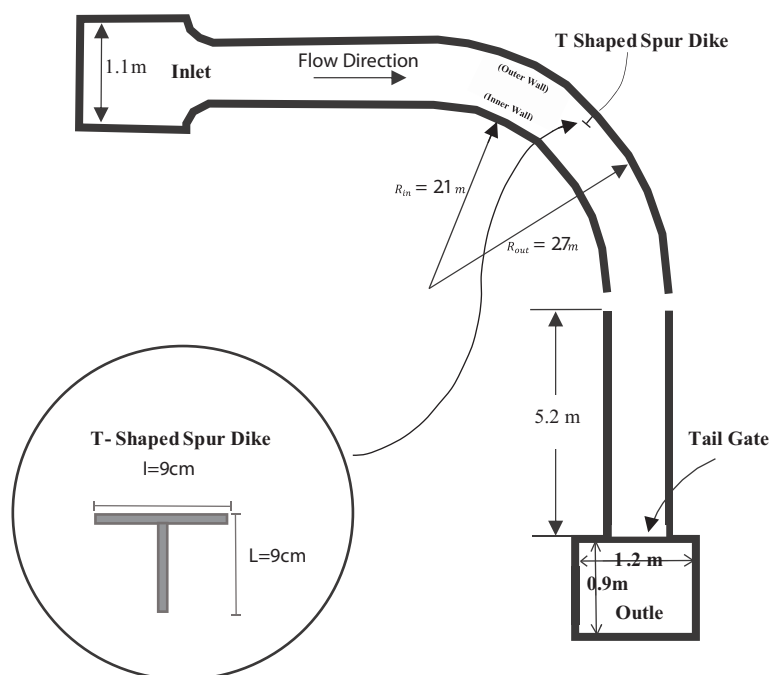

Figure 1. Features of the laboratory flume and schematic view of T-shaped spur dike.

3. Numerical model introduction

FLOW-3D is one of the most powerful software packages concerning fluid dynamics and is developed and supported by Flow Science, Inc. It can do one-, two-, and three-dimensional analysis of flow field and is very much useful in matters of fluids. The governing equations on fluid flow are the continuity equation and momentum equation.

FLOW-3D solves equations governing fluid movement by the finite volume method. The flow environment is divided into a network of steady rectangular cells for each of which there are average values of dependent quantities. In model analysis, the explicit method along with the RNG k-ε turbulence model was utilized. In this software, two numerical methods are used for water surface stimulation: 1-VOF: to show fluid behavior on a free surface. 2-FAVOR: to stimulate surfaces and rigid volumes like boundaries [20]. When modelling a free water surface, the boundary between water and air function VOF (fluid volume F) should follow the governing equation.

For measuring the longitudinal, lateral, and vertical velocity of any point of the flow, a meshing of 42 sections on length, 72 sections on width, and 60 sections on height is used. In Figure 2, a view of the meshing generated by FLOW-3D software is shown in length and width (Figure 2a) and in depth (Figure 2b). As seen in the figure, close to the spur dike, smaller mesh is used because of an increase in gradient. The modelling was carried out for various Froude numbers: 0.2, 0.34, 0.45, and 0.6. Moreover, the height of water is bound to the Froude number, and if the Froude number changes, so does the height of the water. The modelled spur dike is also a 9 × 9 model, and is considered for a 25% submerged spur dike in a 45° position, and a ratio of radius to channel width equal to 4.
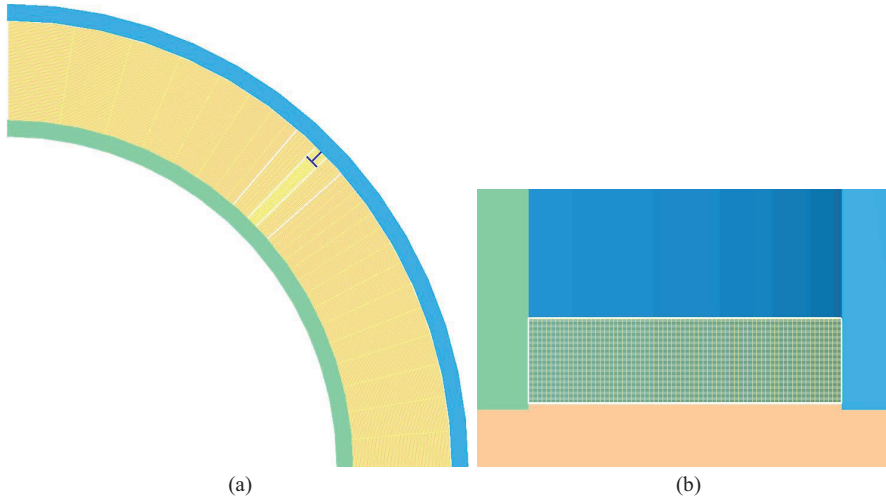

(a)   (b)

Figure 2. A view of the meshing generated by FLOW-3D, a) in length and width; b) in depth.

4. Verification

In order for the results of the numerical modelling to be verified, they are compared with the results of another experiment under the same conditions.

In Figure 3, the spur dike location at the outer bank, different positions of longitudinal sections, and cross sections upstream and downstream of the spur dike are presented.

In Figure 4, the experimental and numerical results pertaining to longitudinal, lateral, and vertical velocity components in cross section, and in a distance of 25% of the length of the spur dike at the downstream (in 45.5° cross section), which is unsubmerged, and a Froude number 0.34 are indicated.

As seen in Figure 4a, away from the internal bend, longitudinal velocity increases, but close to the external bend, it decreases. Furthermore, from the internal bend to the wing of the spur dike, velocities are in the same direction and are the same amount, but from the wing of the spur dike to the external bend, velocity is in an opposite direction and decreases. In Figure 4b, it is observed that away from the internal bend, lateral velocity increases, and the highest velocity is found near the wing of the spur dike. Moreover, from the wing of the spur dike to the external bend, the direction of velocity has changed. As seen in Figure 4c, the maximum vertical velocity is found in the middle of the channel, from the internal bend to the wing of the spur dike. In addition, the highest amount of turbulence is observed between the wing of the spur dike and the external bend. According to these figures, the similarity of the results of FLOW-3D to those of the experiments indicates the verification of data analysis. Based on this, verification of the results from numerical modeling can be achieved.
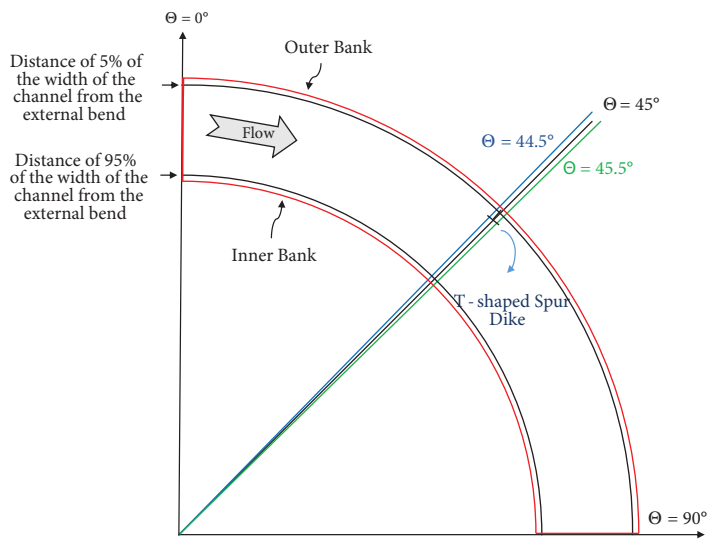
Figure 3. A view of the spur dike location at the outer bank, different positions of longitudinal sections, and cross sections upstream and downstream of the spur dike.
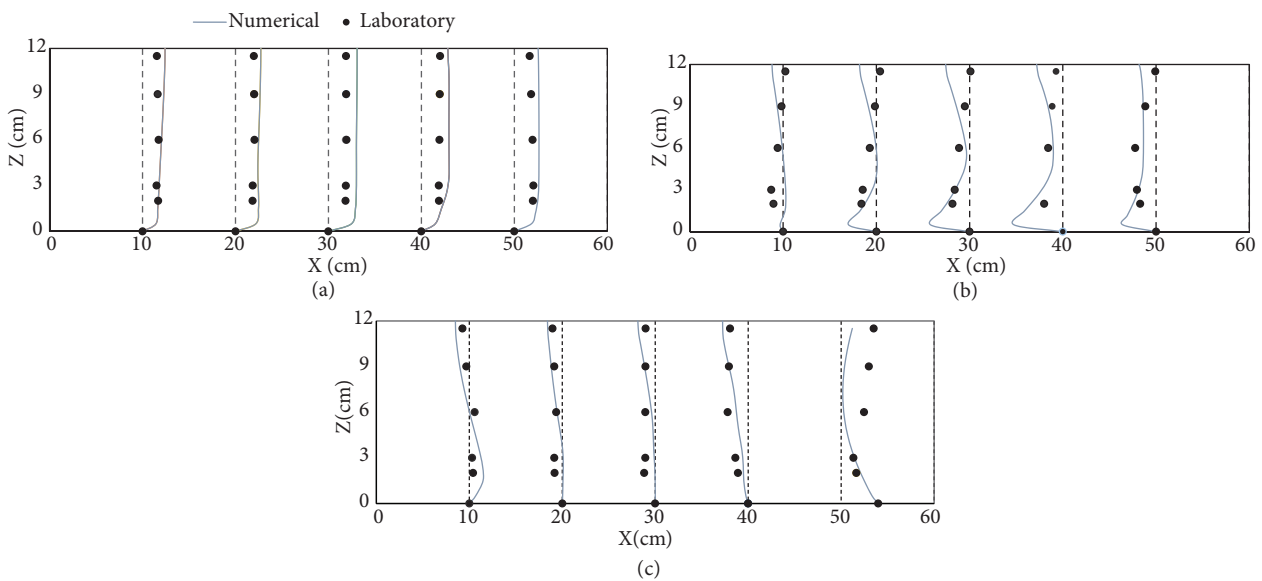

Figure 4. Verification of three-dimensional velocity components in cross section in a distance of 0.25 times the length of the downstream spur dike for Fr = 0.34 and with an unsubmerged spur dike; a) Longitudinal velocity component: 20 cm/s b) Lateral velocity component: 10 cm/s c) Vertical velocity component: 2.5 cm/s.

5. Results

In order to determine the effect of Froude number on the flow pattern around a submerged T-shaped spur dike in a 90° bend, flow patterns in longitudinal, cross, and plan sections were studied, and the results are as follows.

R in these figures represents the distance from the inner bank, Z is the flow depth, Angle refers to the 90° bend angles, and X and Y show the position of the points in the Cartesian coordinate system.

5.1. Study on flow pattern in cross section

As observed in Figure 5, the flow enters the bend and after hitting the web of the spur dike it forms up flow and down flow stream lines, which turn into up flow as Froude number increases. Secondary flow is formed in cross section because of the spur dike's submersion, and water passing over it, and imbalance between centrifugal force and lateral pressure gradient. In addition, due to contraction of the channel section, the stress resulting from the location of the spur dike, and increased velocity of the lateral flow in the zone, vortexes are formed near the inner wall, in the same direction as that of the flow. In Figure 5a, it can be seen that the main secondary flow returns in a distance of 8% of the width of the channel from the internal bend, and merges into the flow moving from the wing of the spur dike towards the bed and the middle of the channel, and forms an anticlockwise vortex as long as 35% of the width of channel. The other secondary flow is also formed near the internal bend. In Figures 5b and 5c, it is observed that the main secondary flow, which has been in the bed of the channel, moves toward the middle, and the top of the channel, while the other secondary flow is diverted toward the bed of the channel. According to Figure 5d, in a distance of 30% of the width of the channel, where the secondary flow is formed, the highest amount of shear stress is observed in the bed of the channel, and with an increase in Froude number the main secondary flow in the middle of the channel moves toward the water surface, while the other secondary flow is diverted toward the bed.
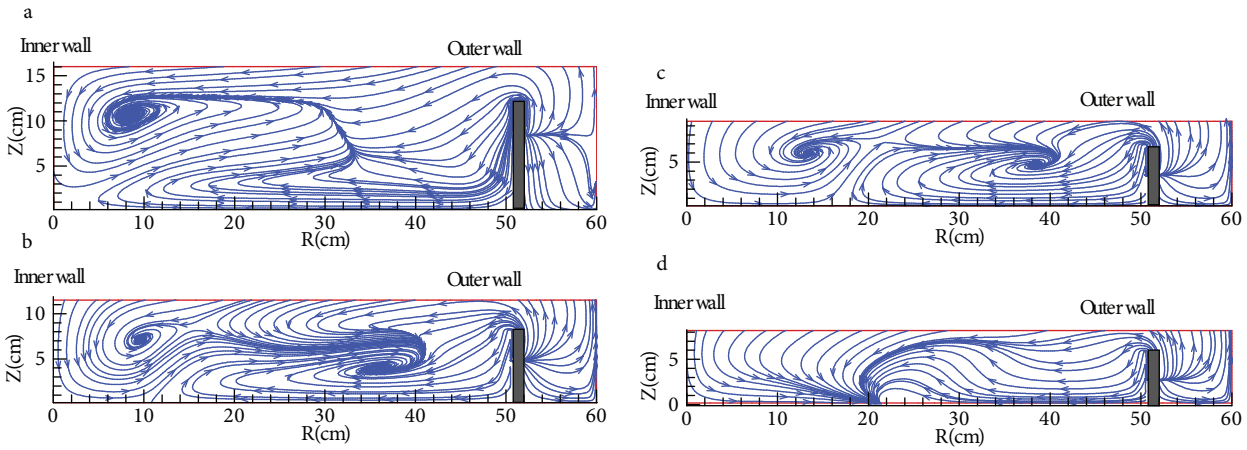

Figure 5. Stream lines in cross section and in a distance of 25% of the length of the spur dike at the upstream, with a 25% submerged spur dike, and different Froude numbers: a) Fr = 0.2 b) Fr = 0.34 c) Fr= 0.45 d) Fr = 0.6.

Moreover, by studying Figure 5, it can be seen that increase in the Froude number causes the location of vortex formation (which is in the distance between the inner wall to the spur dike wing) to move away from the inner wall and approaches the spur dike wing. Therefore, such change in the size of the vortexes results in a 35% decrease in its size.

5.2. Study on flow pattern on longitudinal section

As observed in Figure 6, when the flow enters the bend, and hits the web of the spur dike, with the many velocity changes and pressure difference, it causes the formation of vortexes upstream and downstream of the spur dike. In Figure 6a, it can be observed that the flow upstream of the spur dike hits the spur dike, and forms a clockwise vortex in a distance of 2.5 times the length of the wing of the spur dike. According to Figures 6b–6d there are two reverse flows upstream of the spur dike, one in a distance of 1.25 times the length of the wing and the other in a distance of 2.5 times the length of the wing. In the latter distance, a clockwise vortex
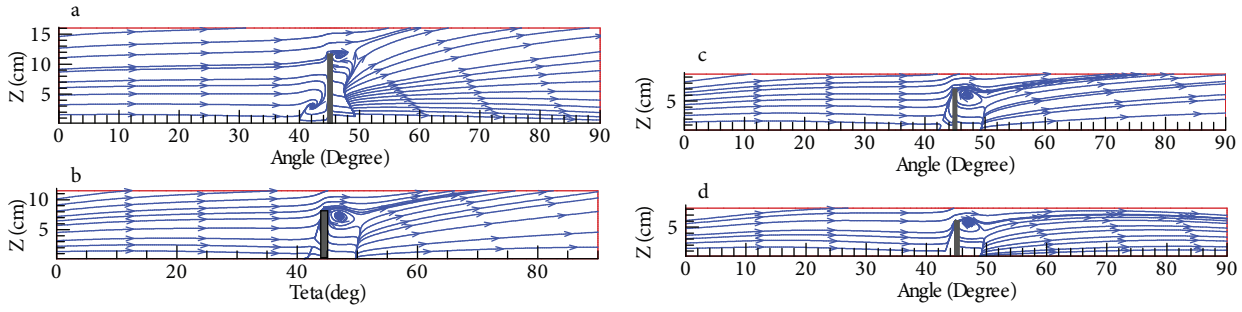
Figure 6. Stream lines in longitudinal section in a distance of 5% of the width of the channel from the external bend, with a 25% submerged spur dike, and different Froude numbers: a) Fr = 0.2 b) Fr = 0.34 c) Fr = 0.45 d) Fr = 0.6.

as big as 2.5 times the wing of the spur dike is formed. As seen, with an increase in Froude number, the flow changes from up flow into straight afterwards.

5.3. Study on flow pattern on plan

As seen in Figure 7, the force resulting from radial acceleration causes a change in velocity distribution in the river section, and also causes a lateral slope on the surface of the water. Therefore, water surface level in the external bend increases. As seen in Figure 7a, when the flow hits the web of the spur dike, a small, anticlockwise vortex is formed upstream. Moreover, lateral flow joins the flow coming from the beginning of the channel upstream, and causes contraction in the section, and pressure on the flow, which leads to a flow separation zone. There is also a helical flow downstream of the spur dike, due to flow circulation and the flow hitting both the outer wall and the wing of the spur dike. When Froude number increases, the flow is joined again after the helical flow. As seen in Figure 7b, the flow hits the spur dike and forms an anticlockwise vortex upstream of the spur dike. A helical flow is also formed downstream of the spur dike, after which the flow is oriented toward the external bend. However, as observed in Figures 7c and 7d, after the vortex is formed upstream and the helical flow downstream, the flow will be of two kinds: one oriented toward the external bend and the other toward the internal bend.

In Figure 8, longitudinal velocity of the flow in plan section for different Froude numbers with a submerged spur dike is shown. The results indicate that at the beginning of the channel, as the Froude number becomes greater, longitudinal velocity also becomes greater; but from the middle of the channel, where the flow reaches the spur dike, to the end of the channel the longitudinal velocity remains constant.

5.4. Three-dimensional components of velocity in cross section

The three-dimensional velocity components of the flow in cross section are presented in Figure 9. As observed in Figure 9a, there is turbulence between the wing of the spur dike and the external bend. Moreover, as the Froude number increases and close to the external bend, longitudinal velocity increases about twice as much as its former value. It is inferred from Figure 9b that, as the Froude number increases, lateral velocity also increases about twice as much as its former value. The greatest velocity is observed in the bed of the channel. It is seen in Figure 9c that vertical velocity near the internal bend to the wing of the spur dike for all Froude numbers is almost the same. Moreover, there are intense variations in the vertical velocity component amounts and turbulence at the distance between the spur dike wing and the outer wall of the channel. Thus, near the outer wall, as the Froude number increases, a 33% decrease in the vertical velocity components variations is observed.
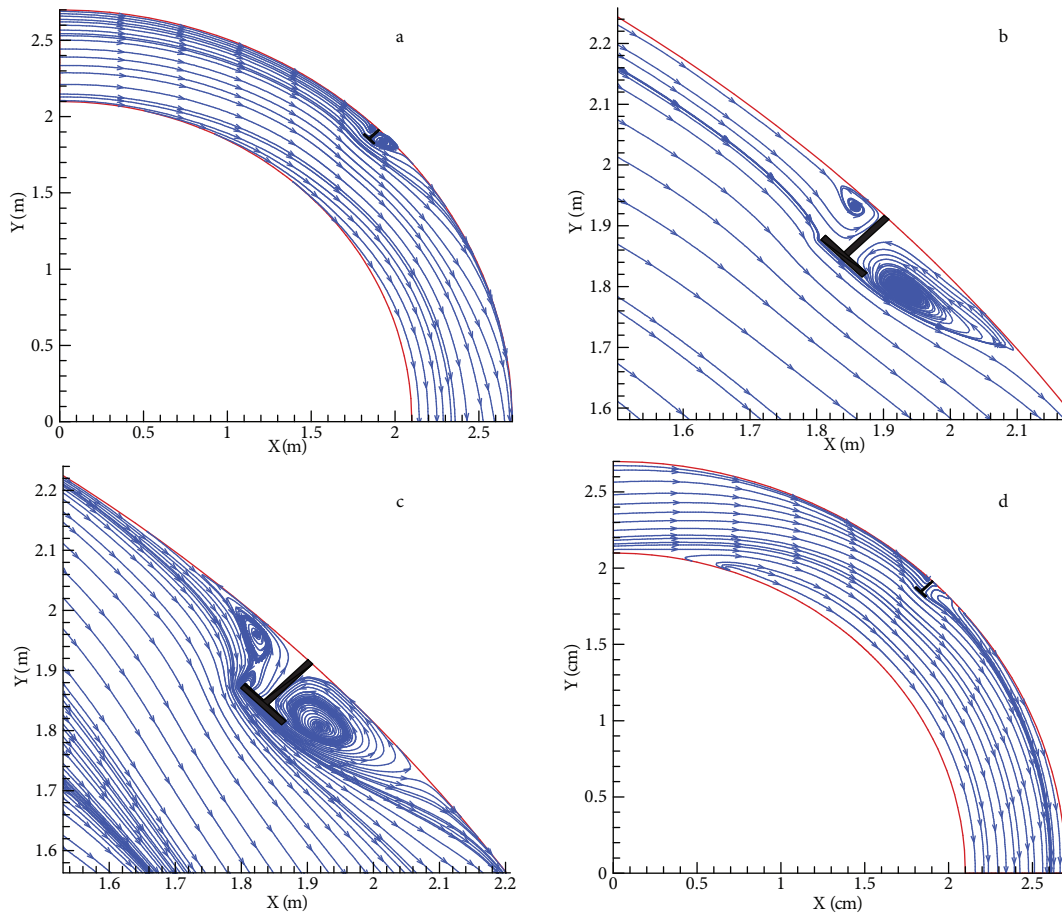
Figure 7. Stream lines in the plan near the bed, with a 25% submerged spur dike and different Froude numbers: a) Fr = 0.2 b) Fr = 0.34 c) Fr = 0.45 d) Fr = 0.6.
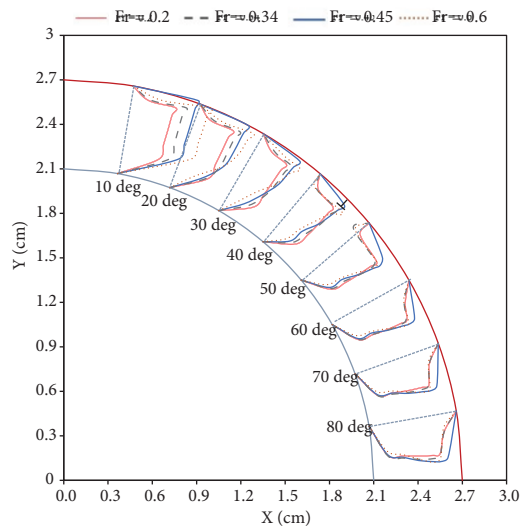

Figure 8. Velocity profile in plan for different Froude numbers, with a 25% submerged spur dike and 50% away from the bed.
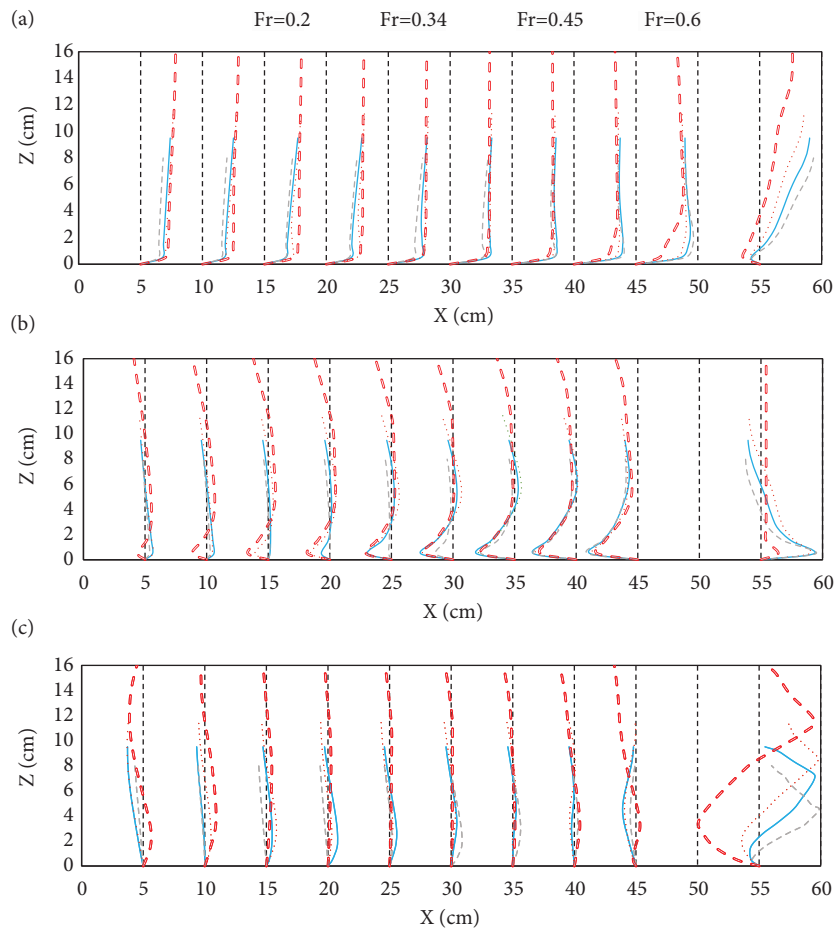
Figure 9. Three-dimensional velocity components in a distance of 0.5 times the length of the spur dike upstream for four different Froude numbers and 25% submerged spur dike; a) Longitudinal velocity component: 20 cm/s b) Lateral velocity component: 10 cm/s c) Vertical velocity component: 2.5 cm/s.

5.5. Length and width of separation zone

As depicted schematically in Figure 10, the flow that passes through the channel changes direction when it hits the spur dike, and after passing the spur dike it joins the external bend. In Figure 11, the width of the separation zone is shown on the vertical axis (h), with different levels of depth on the horizontal axis (z). Analysis indicates that when there are changes in the Froude number for a submerged T-shaped spur dike, there is an increase in changes in the width of the separation zone. In Figure 12, the length of the separation zone at upstream and downstream (the total values of a and b) is shown on the vertical axis, with different levels of depth on the horizontal axis. As observed, when there are changes in the Froude number for a submerged spur dike, changes in length of the separation zone in different levels are negligible.

6. Conclusion

The effect of the Froude number on the flow field around a submerged T-shaped spur dike located in a 90° bend was studied using FLOW-3D software. The numerical results were compared with the experimental results, and the results are as follows:
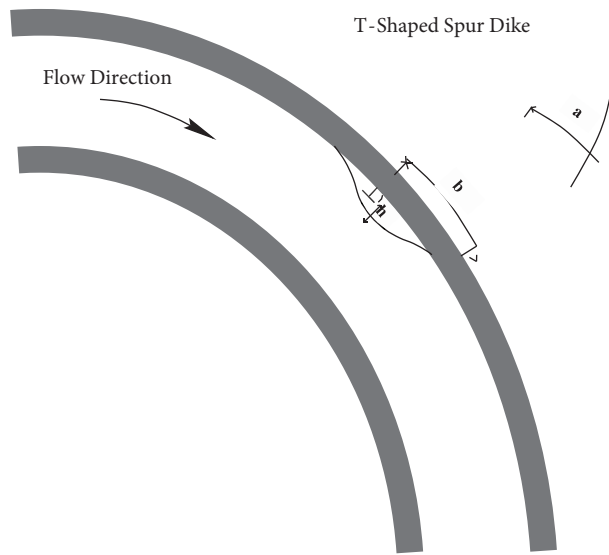
Figure 10. Schematic view of the length, joint, and width of the separation zone.
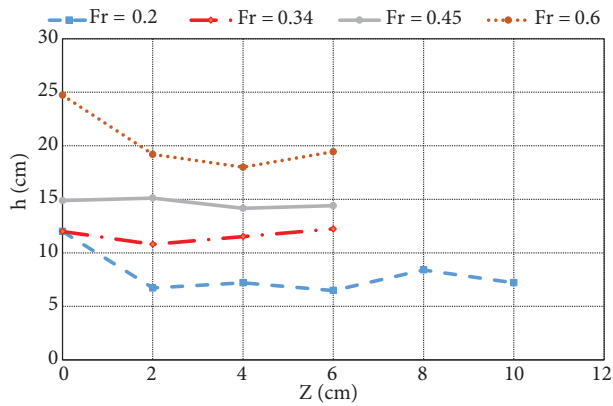

Figure 11. Changes in width of the separation zone of the flow in different levels for different Froude numbers for 25% submerged spur dike.
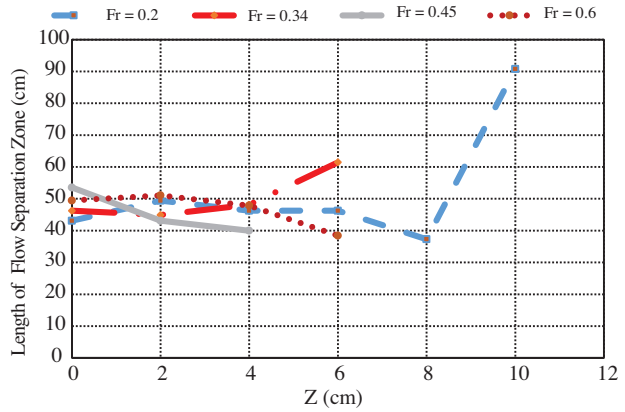

Figure 12. Changes in length of the flow separation zone in different levels for different Froude numbers for 25% submerged spur dike.

1. As the Froude number increases, the flow behind the wing of the spur dike changes from up-down flow into up flow. Furthermore, secondary flows are formed in the width of the channel, and with an increase in Froude number the vortexes become 35% smaller.

2. As Froude number increases, longitudinal and lateral velocities become about twice as much as their former value. Moreover, the further distance from the internal bend, the more lateral velocity in the bed of the channel.

3. The highest amount of vertical velocity is observed between the wing of the spur dike and the external bend, and closer to the external bend, with an increase in Froude number, the vertical velocity components variations decrease by 33%.

4. Study on the vertical velocity component in cross section around the spur dike indicates that getting close to the wing of the spur dike, in a distance of 10% of the width of the channel, and from the wing of the spur dike, the flow becomes turbulent, and getting close to the external bend leads to smaller turbulence.

5. Width of the separation zone for a submerged T-shaped spur dike increases when Froude number changes. When Froude number changes, there is no change in the length of the separation zone of the flow for this spur dike in different levels.

Nomenclature

B   flume width;
Fr   Froude Number;
L   length of the wing of the spur dike;
l   length of the web of the spur dike;
Z   depth of water;
U   velocity component in the x-direction;

V   velocity component in the y-direction;
W   Velocitiy component in the z- direction;
a   length of separation zone at upstream of spur dike;
b   length of separation zone at downstream of spur dike;
h   width of separation zone;

References

[1] Kuhnle RA, Jia Y, Alonso CV. Measured and simulated flow near spur dikes. US-China workshop on advanced computational modeling in hydroscience and engineering, Oxford, MS, USA: 2005

[2] Ahmad M. Spacing and protection of spurs for bank protection. Civil Engineering and Publication Review 1951; 46: 3–7.

[3] Ahmad M. Experiments on design and behavior of spur dikes. Proc. Int. Hyd. Convention, New York, NY, USA: ASCE; 1953. pp. 145–159.

[4] Gill MA. Erosion of sand beds around spur dikes. J Hydr Div 1972; 98: 91–98.

[5] Rajaratnam N, Nwachukwu BA. Flow near groin-like structures. J Hydraul Eng-ASCE 1983; 109: 463–480.

[6] Rajaratnam N, Nwachukwu BA. Erosion near groin-like structures. J Hydraul Res 1983; 21: 277–287.

[7] Soliman MM, Attia KM, Kotb Talaat AM, Ahmed AF. Spur dike effects on the river Nile morphology after high Aswan dam. Congress of the International Association of Hydraulic Research, Vol. 120, San Francisco, CA, USA: IAHR; 1997. pp. 125–146.

[8] Blanckaert K, Graf WH. Mean flow and turbulence in open-channel bend. J Hydraul Eng-ASCE 2001; 127: 835–847.

[9] Booij R. Measurements and large eddy simulations of some curved flumes. J Turbul 2003; 4: 1297–1313.

[10] Giri S, Shimizu Y, Surajate B. Laboratory measurement and numerical simulation of flow and turbulence in a meandering-like flume with spurs. Flow Meas Instrum 2004; 15: 301–309.

[11] Nagata N, Hosoda T, Nakato T, Muramoto Y. Three-dimensional numerical model for flow and bed deformation around river hydraulic structures. J Hydraul Eng-ASCE 2005; 131: 1074–1087.

[12] Fazli M, Ghodsian M, Saleh Neyshabouri, AA. Scour and flow field around a spur dike in a 90° bend. Int J Sediment Res 2008; 23: 56–68.

[13] Ghodsian M, Vaghefi M. Experimental study on scour and flow field in a scour hole around a T-shaped spur dike in a 90° bend. Int J Sediment Res 2009; 24: 145–158.

[14] Duan J. Mean flow and turbulence around a laboratory spur dike. J Hydraul Eng-ASCE 2009; 135: 803–811.

[15] Yazdi J, Sarkardeh H, Azamathulla HM, Ghani AA. 3D simulation of flow around a single spur dike with free-surface flow. International Journal of River Basin Management 2009; 8: 55–62.

[16] Vaghefi M, Ghodsian M, Salehi Neyshabori SAA. Experimental study on the effect of a T-shaped spur dike length on scour in a 90 degree channel bend. Arab J Sci Eng 2009; 34: 337–348.

[17] Vaghefi M, Ghodsian M, Salehi Neyshabori SAA. Experimental study on scour around a T-shaped spur dike in a channel bend. J Hydraul Eng-ASCE 2012; 138: 471–474.

[18] Vaghefi M, Ghodsian M, Adib A. Experimental study on the effect of Froude number on temporal variation of scour around a T-shaped spur dike in a 90 degree bend. Appl Mech Mater 2012; 147: 75–79.

[19] Acharya A, Acharya A, Duan J. Three dimensional simulation of flow field around series of spur dikes. International Refereed Journal of Engineering and Science (IRJES) 2013; 2: 36–57.

[20] Flow Science. FLOW-3D User's Manual. 9.3 editions, USA: Flow Science, Inc. 2008.